ACS OMEGA

http://pubs.acs.org/journal/acsodf

Article

Analysis of Aging Products from Biofuels in Long-Term Storage

Karin Engeländer, Anton Duchowny, Bernhard Blümich, and Alina Adams*

Cite This: *ACS Omega* 2022, 7, 26256−26264

Read Online

ACCESS | Metrics & More | Article Recommendations | Supporting Information

ABSTRACT: The long-term aging processes during storage of different heating oils and their blends with biofuels including fatty acid methyl ester, hydrogenated vegetable oil, and power-to-liquids products were followed by different analytical techniques, and the aging products were analyzed. While most standard techniques are time-consuming and labor-intensive and specify only a single property, analyses by benchtop nuclear magnetic resonance spectroscopy proved to be effortless and fast. Moreover, only 0.4 mL of the sample is required for nondestructive NMR measurements. White and waxlike precipitates were found in FAME stored at a cold temperature and identified as esters of glycerol with saturated side chains by chromatographic, thermal, and spectroscopic analyses. At colder temperatures, they reversibly precipitate and can lead to system failure.

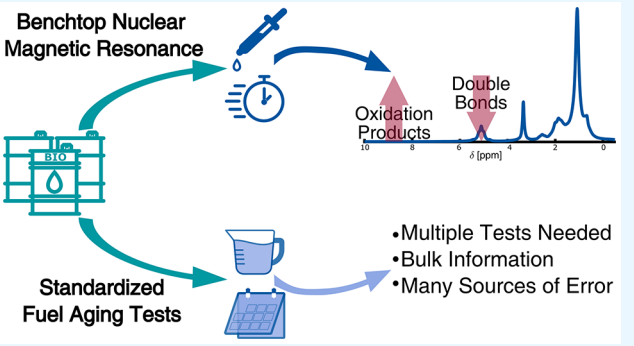

INTRODUCTION

For decades, CO_2 emission reduction has been a key topic in the research of regenerative liquid fuels.[1,2] The first regenerative fuels introduced into the market were mixed with petro-based fuels like, e.g., ethanol in gasoline and fatty acid methyl esters (FAMEs) in diesel and heating oil. FAMEs are generated from vegetable oil by transesterification with methanol,[3] although algae can serve as a resource as well.[4] Even though biofuels were introduced several years ago, their aging behavior is still thoroughly discussed up to this day.[5] FAME blends are known to have lower oxidation stability than pure fossil heating oil and, thus, require additives for stabilization.[6,7] During extended storage or under the impact of heat, irradiation, or friction, oxidation reactions lead to various oxygenated products and oligomers.[8−10] Depending on the FAME concentration, these products form sediments.[11,12] In addition to being complex natural products themselves, FAME fuels and blends also contain a multitude of contaminants, which participate in the sedimentation process.[13,14] Moreover, the relation between sediment formation and FAME content is not linear owing to the sediment's solubility.[15] Higher FAME concentrations can keep oxidation products dissolved, but the polarity is insufficient in lower concentrated FAME blends. Several studies have focused on the influence of FAMEs in transportation applications, especially concerning deposit formation in diesel injectors or exhaust emission.[10,11,16−18] However, they paid no attention to how these aging products formed and could be prevented. Instead, only the measurable effects on injection parameters and emissions were observed.

Although standardized fuel testing methods can determine parameters like density, oxidation stability, or sediment formation, they are time-consuming and labor intensive. Different methods need to be combined because each method specifies only a single property, resulting in considerable fuel quantities being required for analyses. The rapid development of new alternative fuels, such as hydrogenated vegetable oil (HVO) or synthetic power-to-liquid (PtL) fuels, implies numerous tests of their long-term properties and performance as pure and blended fuels. In the PtL process, renewable energy is used to produce hydrogen gas, which reacts with carbon dioxide to form a broad range of chemicals, e.g., liquid fuels, also referred to as e-fuels.[19] To this end, benchtop nuclear magnetic resonance (NMR) spectroscopy is employed alongside well-established standard oil testing methods. So far, benchtop NMR was mainly utilized for time-domain analyses.[20−22] However, the examination of NMR signals in their time domain can only provide physical information about the sample, while chemical information can be obtained by the analysis of the frequency domain of NMR signals.[23−26] Compared to the conventional high-field NMR instruments, benchtop spectrometers are smaller in size, less expensive, and do not necessarily require sample preparation or specialized personnel for operation and, thus, can provide the benefits of

Received: March 31, 2022
Accepted: June 15, 2022
Published: July 18, 2022

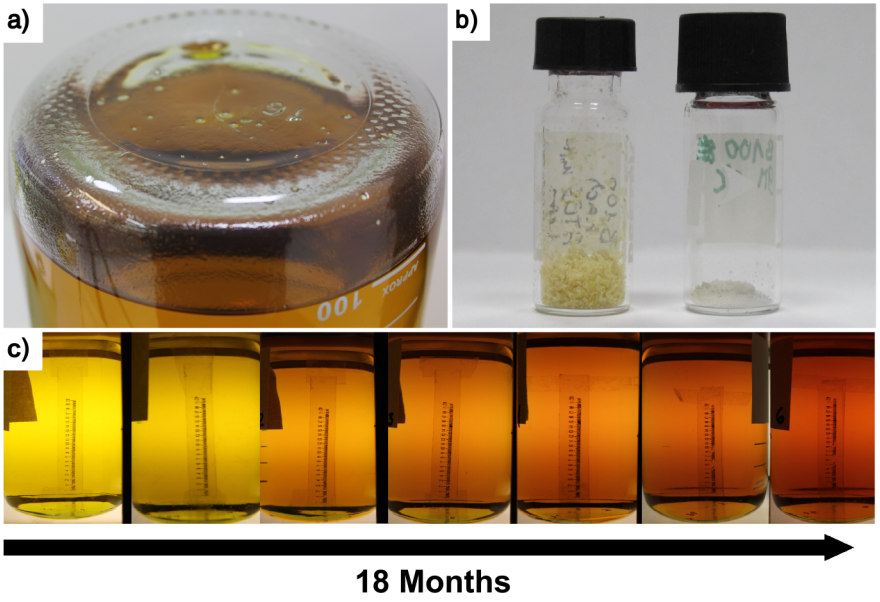

Figure 1. Photograph of the precipitates formed during cold storage. (a) Sticking to the bottom of a B20 glass bottle after 3 months of storage at 8 °C. (b) After filtration on a cellulose nitrate filter. (c) Darkening of B20 oil during long-term storage observed when photographed in a photo booth. Adapted with permission from ref 34. Copyright 2020 DGMK e.V.

NMR spectroscopy with low effort. Moreover, benchtop NMR spectroscopy requires only about 0.4 mL of sample volume, which is far less than that for the standardized methods, and is capable of examining complex molecules and mixtures.[27−29]

In this work, bioheating oils according to DIN SPEC 51603-6, FAMEs according to EN 14214, and blends of these were stored for 18 months at 8 and 40 °C. Subsequently, oils and aging products were examined by various standardized analytical methods and NMR. Furthermore, solid precipitates were extracted from some fuels stored at 8 °C and examined by NMR and infrared (IR) spectroscopy, two-dimensional gas chromatography coupled with mass spectrometry (2D-GC-MS), as well as thermal analysis, i.e., differential scanning calorimetry (DSC) and thermogravimetric analysis (TGA). So far, both DSC and TGA have been used to examine liquid fuels exposed to high temperatures for a short period[30−33] but not for solid aging products. The multitude of analytical methods gives detailed insight into fuel aging during long-term storage and allows the evaluation of how benchtop NMR can reduce the workload for obtaining fuel properties.

EXPERIMENTAL RESULTS

Photographic and Visual Inspection. The complete photo spreads can be found in Supporting Information Table S1. Except for P100 and H100, which stayed transparent the whole time, all oils darkened during long-term storage. Oils stored at 8 °C darkened less than the same oils stored at 40 °C, showing a temperature-dependent aging effect. B100 darkened rapidly during the first 12 months but lightened up afterward. However, color changes are less noticeable by visual inspection. White precipitates in flakes or spheroids were found in B100 after 3 months and B20 after 6 months of storage at 8 °C. Some were floating in the oil, while others stuck to the bottom of the bottle, as shown, for example, in Figure 1a. Once the oil reached room temperature, the precipitates disappeared. After all analyses were performed, leftover oil was retained at 8 °C and formed this kind of precipitate as well. That was even the case for B100, which did not show precipitates at 40 °C. B20 bottles containing additives did not form precipitates. It was possible to isolate the substance by filtering the cold oil on a cellulose−nitrate filter and washing off residual oil with *n*-heptane (Figure 1b).

Analysis of Aged Oils. *Standardized Methods.* The complete overview of the standard methods' results is listed in Supporting Information Tables S2−S9. In the following, the most significant results are discussed, and a brief summary of all standardized tests can be found in Table 1.

Table 1. Main Findings of the Different Standardized Analytical Techniques in the Long-Term Storage Experiment

method	concluding results
density	small increase for fuels stored at 40 °C (largest +0.88% for B100) while <0.05% change at 8 °C
total contamination	most values below the detection limit (10 mg kg^{-1})
storage stability	all values below 30 mg kg^{-1}
thermal stability	all values below 35 mg kg^{-1}
oxidation stability	except for P100 all values decrease
acid number	inconsistent, fluctuating results with some samples exceeding the critical value (0.25 mg KOH g^{-1})
water content	below 100 mg kg^{-1}, except for B100 (close to 1000 mg kg^{-1})

The density of all examined oils stored at 40 °C increased with the storage time, whereas oils stored at 8 °C showed no significant change as laid out in Table S2. Figure 2a depicts the normalized densities of selected oils for better visual comparison, with the other fuels shown in Figure S1a. The most notable increase was observed for B100 stored at 40 °C, whose density changed by almost 1%, with most of the rise occurring in the last 6 months. Contrary to B100, the density changes are similar for the other oils, with less change as storage time progresses. Moreover, H100, P100, and their blends have the lowest density change. Nevertheless, all

https://doi.org/10.1021/acsomega.2c01970
ACS Omega 2022, 7, 26256−26264

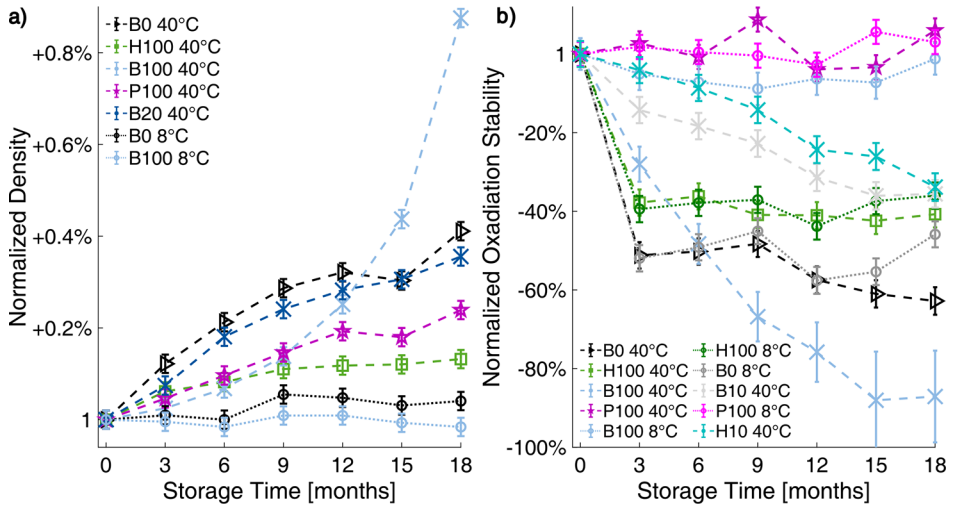

Figure 2. Change of (a) density and (b) PetroOxy oxidation stability over the long-term storage. Values were normalized to values of the nonaged oil for better visualization. Oils stored at 8 °C are depicted with dotted lines and circles, whereas dashed lines are used for oils stored at 40 °C.

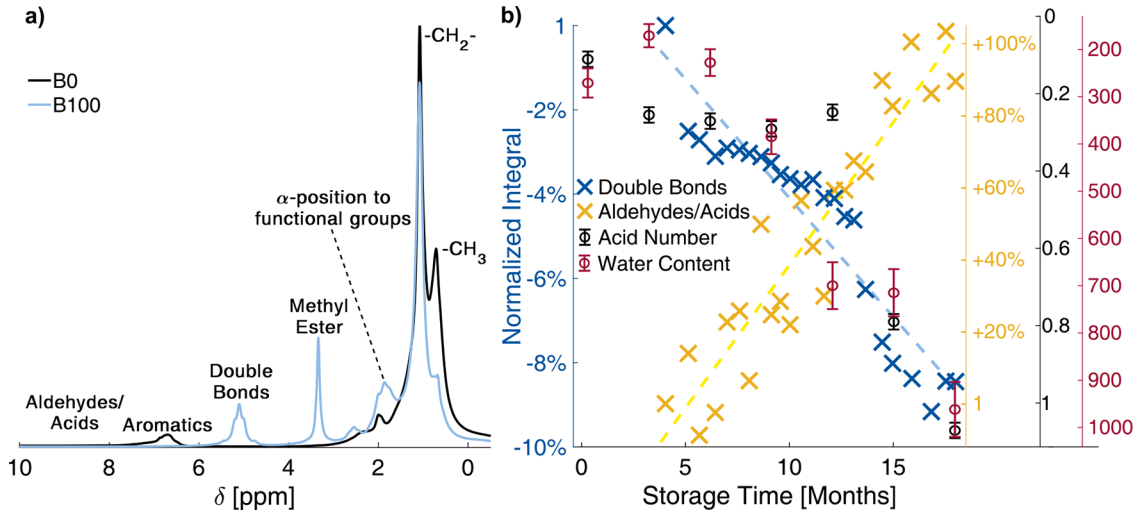

Figure 3. (a) 43 MHz ^{1}H NMR spectra of B0 and B100. (b) Property changes of B100 during long-term storage: NMR integral of double bonds (left *y*-axis, blue), aldehydes and acids (right *y*-axis, orange), the acid number (right *y*-axis in mg KOH g^{-1}, black, reversed), and the water content (right *y*-axis in mg kg^{-1}, red, reversed).

obtained values are within the corresponding measurement norm and, therefore, not critical.

The normalized results of the PetroOxy oxidation stability test are shown in Figure 2b and Figure S1b, whereas the original number values are given in Table S3. The synthetic power-to-liquid fuel P100 shows much larger oxidation stability than the other blends (263.6 min induction time) and, moreover, is the only sample that does not lose oxidation stability over time at both storage temperatures. On the other hand, the oxidation stability of B0 and H100 (both stored at 40 °C) suffers significantly in the first 3 months. It stays relatively constant at longer storage times for H100, while it further decreases for B0 but at a much lower rate. Furthermore, there is hardly any difference between B0 or H100 stored at 8 and 40 °C. B100 stored at 40 °C shows a continuous decrease over the full observed time frame and, additionally, has the lowest oxidation stability of all examined species to begin with (43.8 min induction time). Its induction time reaches close to 0 min when stored at 40 °C for 18 months but hardly loses any of its initial stability when stored at 8 °C. This behavior suggests that B100 indeed suffered from oxidation while being kept at 40 °C, although this is still a relatively mild storage environment. Intriguingly, FAME and HVO blends perform better than their corresponding pure components, despite the relatively low concentration of 10% or 20% alternative fuel in heating oil extra light (HEL). P10 also loses far less oxidation stability than HEL, but its performance is comparable to that of other blends (Figure S1). As B100 oxidation advances, its water content increases significantly and exceeds the critical value for FAMEs of 500 mg kg^{-1} (EN 14214) by nearly 100% after 12 months (Table S4) with almost 1000 mg kg^{-1} at the end of the storage period. The critical water contents of HEL and HEL blends with alternative fuels are 200 mg kg^{-1} (DIN 51603-1) and 300 mg kg^{-1} (DIN 51603-6), respectively.

Concerning pure B20 and the two samples treated with additives, the results show that the use of small amounts of additives is already capable of improving properties such as density (Table S2), PetroOxy oxidation stability (Table S3), and thermal stability (Table S5). In contrast, total contamination (Table S6), storage stability (Table S7), and acid

https://doi.org/10.1021/acsomega.2c01970
ACS Omega 2022, 7, 26256−26264

number (Table S8) stay nearly the same. Yet, the oxidation stability as measured by the rancimat method (Table S9) showed inconclusive results that the PetroOxy experiments did not reproduce. Here, the initial oxidation stability of B20 with Add1 is lower and B20 with Add2 higher than of pure B20. While pure B20 and B20 with Add2 continuously lose stability, the oxidation stability of B20 with Add1 increases in the first 6 months, although a continuous decrease would be expected.

In summary, the standard analytical methods can work out differences between the oils and jointly draw a similar picture, in that B100 stored at 40 °C experiences the most noticeable change of its properties and sometimes exceeds the threshold limits defined by the norms. However, as can be seen by Tables S2−S9, extensive labor effort and fuel volume are required compared to the retrieval of essential information.

^{1}H NMR Spectroscopy. Figure 3a depicts the ^{1}H spectra of B0 and B100 along with the assignment of the signals of interest. Table S10 lists a more comprehensive chemical shift assignment. Integration of the different peaks allows the quantification of the concentration of the corresponding functional groups. Integrals from selected ranges in the ^{1}H NMR spectra of all samples containing FAMEs except B10 showed a significant trend according to the Neumann trend test (Table 2). However, integral changes with aging time are relatively small, and only B100 shows changes of more than 5% in the double-bond and aldehyde and acid regions. B100 loses nearly 9% of the signal in the double-bond region, seemingly in a stepwise manner as depicted in Figure 3b. The stepwise reactions were also captured photographically, with different degrees of coloration during the storage period (Table S1). Meanwhile, a continuous formation of aldehydes or acids is observed, contributing 0.14% of the total integral after 18 months of storage at 40 °C. The acid number experiments reveal a stepwise increasing acid content, which matches the decreasing double-bond integral well when the acid number *y*-axis is reversed. Moreover, the water content also abruptly increases, albeit a little bit earlier than the NMR integral and acid number.

Furthermore, all B20 samples lost some aromatic structures, while both B20s treated with additives simultaneously showed an increase in double bonds (Table 2). Pure B0, HVO, PtL, and their blends did not show any change in the spectra during the observed storage period. Thus, storage of such fuels over a long time is feasible, whereas FAME and its blends are less stable. However, R33 and B10 with 7% and 10% FAME, respectively, did also not show significant trends in the NMR spectra, indicating that a low FAME content is not critical for the long-term stability of a blend.

Table 2. Integral Changes in ^{1}H NMR Spectra during the Long-Term Storage

fuels and spectral region	Neumann trend test significance level (%)	integral change over observed time frame (%)
B20 (5.8−8.1 ppm)	99.20	−1.7
B20 (1.7−2.2 ppm)	99.99	−4.1
B20 + Add1 (6.1−8 ppm)	99.00	−3.0
B20 + Add1 (4.6−5.6 ppm)	99.50	+3.5
B20 + Add2 (6.1−7.9 ppm)	99.90	−3.8
B20 + Add2 (4.6−5.7 ppm)	97.00	+1.7
B100 (8.7−9.8 ppm)	99.99	+121.4
B100 (4.6−5.6 ppm)	99.99	−8.9

Thermal and Structural Analysis of the Solid Precipitate. Thermal analytical methods were used to examine the precipitate because they require only around 5−10 mg of sample. Whereas TGA depicts the sample's devolatilization behavior by measuring mass loss during heating, DSC measures heat flux and can visualize endothermic or exothermic processes. For TGA analysis, precipitates from B100 were compared to the original oil in Figure 4a. The B100 oil hardly loses mass until 150 °C with a rapid mass loss at around 200 °C, independently of whether it is flushed with nitrogen or oxygen. However, at ∼250 °C, around 20% of the original mass remains in the oxygen atmosphere, while hardly any sample remains in the nitrogen atmosphere. The residual 20% of mass slowly evaporates up to a temperature of 480 °C. This indicates that FAME can react with oxygen to form residues that require extremely high temperatures to burn off, which are not reached in a real-world burner system. However, such residues were not formed during the long-term storage at 40 °C.

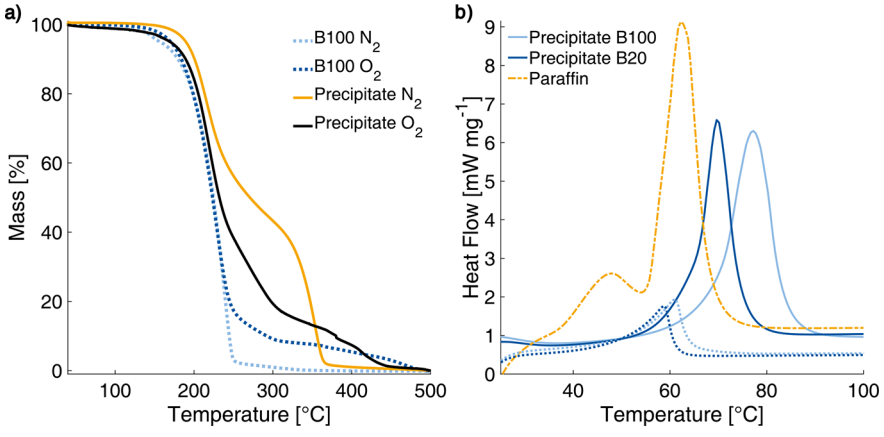

Figure 4. (a) TGA measurements in the O_2 and N_2 atmosphere of fresh B100 oil and precipitates found during long-term storage. (b) DSC curves of precipitates (solid line) of B20 and B100 in comparison with a commercial paraffin (dashed line). Dotted lines show the precipitate's second heating cycle.

https://doi.org/10.1021/acsomega.2c01970
ACS Omega 2022, 7, 26256−26264

The precipitates of B100 show a different behavior. Below 200 °C, the curves of the oil and precipitate are close together. The mass loss is retarded in the nitrogen atmosphere, whereas in oxygen it continues, albeit slower than for the B100 oil. At ∼320 °C, however, the sample purged in nitrogen rapidly evaporates until hardly any residues are left at ∼360 °C. The sample purged in oxygen continues to lose mass slowly up to 450 °C. The data suggests the white precipitate found in the samples containing FAME stored at 8 °C consists of molecules with a vapor pressure lower than that of the original oil but still having the same capability of reacting with oxygen to form residues that are hard to burn off. The slower devolatilization of B100 in oxygen, in conjunction with the increasing density and decreasing oxidation stability over time, indicates that B100 integrates oxygen into its molecules. However, the physical properties change only moderately during storage as shown by the standardized methods. Nevertheless, this can cause complications in real-world burner components where the oil is exposed to higher temperatures.

DSC analyses were performed on solid precipitates originating from B20 and B100 and compared to commercially available paraffin with a melting point of 59 °C according to the manufacturer. Paraffin was chosen for this comparison because of its close resemblance to the precipitate. The thermograms of the precipitates in Figure 4b shows crystalline structures with a melting point between 70 and 80 °C with a unimodal shape. The peaks are still present in the second heating cycle, indicating a reversible crystallization. Moreover, the melting behavior of the precipitate and paraffin, defined as carbohydrates with a chain length between 20 and 40, is different. While paraffin shows two peaks during heating, corresponding to a solid−solid and solid−liquid transition,[35] the precipitate has only one peak with a significantly higher melting point. These differences in melting behavior indicate that the precipitates contain polar structures, leading to higher melting points. If reversible crystalline structures with a melting point between 70 and 80 °C were formed solely by van der Waals forces, the carbon chain length would need to be larger than 30 (melting point of dotriacontane: 69 °C). This is unlikely in the given case as FAME was produced from canola seed oil, the fatty acids of which range between 16 and 20 carbon atoms. Complementary IR data from precipitates found in B20, shown in Figure 5, confirms the presence of polar molecules. However, the signals below 2000 cm^{-1} cannot be attributed to FAMEs or long-chained carbohydrates alone, indicating the involvement of other substances as well.

Compared to the base oil, the precipitate's ^{1}H NMR spectrum in Figure 6a lacks signal intensity in the double-bond region at around 5.5 ppm and the corresponding aliphatic region around 2 ppm marking the neighboring aliphatic groups. However, three additional signals can be observed in the region between 3.7 and 4.2 ppm, which cannot be attributed to FAME or one of its aging products. Instead, these signals match NMR spectra from substituted glycerols.[36] The FAME methyl-ester peak at 3.7 ppm is still present but overlaps with one of the glyceride peaks. Since the precipitate had been washed multiple times during the filtration using *n*-heptane, this FAME residue is either chemically bound to the precipitate or entrapped inside the solid structures until they are dissolved with *d*-chloroform. Thus, the NMR results indicate the presence of glycerides, mono- and disubstituted with long and mostly saturated carbohydrate chains, capable of binding FAMEs.

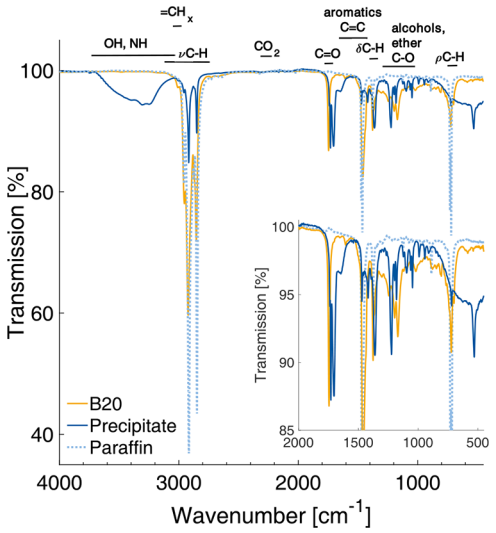

Figure 5. Comparison of infrared spectra from B20 oil, precipitate found in cold-stored B20, and commercial paraffin.

According to the 2D-GC-MS measurements, the precipitates of B100 consist mainly of FAME. Additionally, monoglycerides, oxidized FAME, phthalates, and long chains of alkanes were found. 2D-GC-MS measurements revealed conclusively that the precipitates from the cold-temperature storage are complex mixtures. However, only a small fraction is made up of molecules that can be associated with FAME that underwent a chemical reaction.

SUMMARY OF RESULTS

During storage at 40 °C, the oil's density increased. Generally speaking, an increase of density could be associated with the evaporation of small molecules. For oils, however, these should make up only a modest part of the original oil matrix. Yet, aging products, e.g., originating from oxidation,[37] could fall into this category. Due to processing and purification, oxidation products may be present even in freshly produced FAME. An indication could be that 2D-GC-MS found short-chained alkanes in FAME stored at 8 °C, where it did not show signs of aging like the same fuel stored at 40 °C. Alternatively, oligomerization or polymerization can also cause the density to increase. However, neither NMR, DSC, or 2D-GC-MS suggested a significant formation of high molecular weight molecules, contrary to findings when fuel is exposed to high temperature.[38,39] Hence, the increase in density during long-term storage is influenced mainly by the evaporation of small molecules and can be associated with oxidation.

As shown by the oxidation stability, the acid number, and NMR measurements, B100 continuously oxidizes at 40 °C. This is also reflected in the density measurement, where B100 is the only fuel for which density changes more rapidly over time, i.e., more small oxidation products are being formed and evaporate. Meanwhile, density change decreases over time for all other examined fuels and blends. Comparison of the NMR signal strength of acids and aldehydes with the acid number measurements shows some differences. Although both show an increasing content of acidic groups, the increase is linear for NMR and stepwise for the acid number. Moreover, the rise is less pronounced according to NMR, and the stepwise increase seems to follow the same timing as the decrease of the NMR double-bonds signal and the darkening in photographic

https://doi.org/10.1021/acsomega.2c01970
ACS Omega 2022, 7, 26256−26264

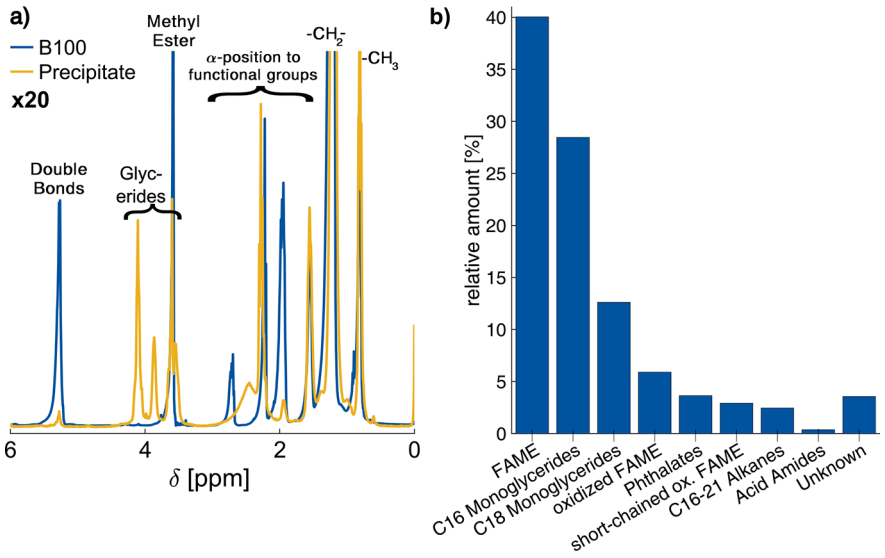

Figure 6. (a) Comparison of ^{1}H NMR spectra from B100 oil and the precipitate found during cold-temperature storage dissolved in *d*-chloroform. (b) Quantitative molecular precipitate composition according to 2D-GC-MS.

inspection. Whereas the acid number quintuples, the NMR signal only doubles, which is partially due to the fact that NMR data was only available 4 months after the storage experiment was started. Furthermore, acidic groups dissociate rapidly, making their signal difficult to capture by NMR. Conventional high-field NMR requires the utilization of deuterated solvents, which most often impedes acquiring signals from acids and alcohols. Nevertheless, with benchtop NMR it is simple to acquire these signals but at the expense of sensitivity.

NMR data showed that all B20 samples lost signal in the aromatic region, implying an interaction between FAMEs and aromatics. A similar conclusion could be drawn from the work of Jose and Anand (2016), where a mixture of a FAME with high unsaturated content and petrofuel was less stable than when mixed with another FAME having a low content of unsaturated carbon chains.[40]

Both NMR and 2D-GC-MS found substituted glycerides in the precipitate occurring during cold storage. However, it is doubtful that they are an aging product. It is more likely that those are residues from the FAME production, which have not fully undergone the transesterification with methanol. Alternatively, residual glycerol may have reacted in a reverse transesterification to produce these products.[37] Together with aging products and FAMEs, the glycerides accumulated at 8 °C to clusters visible by eye but dissolved again once the fuel or blend reached room temperature.

Consequently, the storage of FAME and FAME blends at elevated temperatures results in fuel aging, which for B100 accelerates as time progresses. Storing such fuels at lower temperatures, however, leads to macroscopic precipitates capable of clogging up filters or fuel lines in a burner system.

CONCLUSION

Traditional heating oil and the alternative liquid fuels HVO, PtL, and FAME were stored as pure oils and as blends at 8 or 40 °C for 18 months. In the standard testing methods, B100 exceeded critical limits of acid number and water content defined by the respective norms. For the other tests, it showed clear trends toward inferior values when stored at 40 °C. The PtL fuel, or e-fuel, a Fischer−Tropsch synthesis product based on renewable energy, proved to be exceptionally stable during this experiment. Although they deliver insightful information, the standardized methods only specify one criterion. Hence, multiple standardized tests are required for estimating a fuel's quality, resulting in an elaborate workload and a plenitude of data. Benchtop ^{1}H NMR spectroscopy was able to quantitatively follow the depletion of double bonds and the formation of oxidation products in biofuels with minimal operational effort and measurement time. Hence, this method can be utilized to measure fuel composition and quality.

During cold storage, precipitates were found in B20 and B100 and characterized by various methods. Both the 2D-GC and the NMR measurements indicated saturated FAMEs and substituted glycerides with saturated side chains in the precipitates. This outcome is consistent with the DSC results that detected crystalline structures, preferably formed by saturated rather than unsaturated carbohydrate chains. Both DSC and IR experiments indicated the presence of polar structures, further endorsing these findings. The glycerides accumulate and precipitate reversibly at low temperatures. However, precipitates only occurred in samples with at least 20% FAME and without additives, indicating that aging products play a role in this process, presumably due to polarity changes in the sample. Since, apparently, transesterification of glycerides with saturated side chains is less effective, proper purification after FAME production could prevent precipitates potentially leading to system failures. Furthermore, when HEL is blended with a FAME, a FAME content below 20% should be chosen, as B10 showed only marginally worse properties than B0.

EXPERIMENTAL SECTION

Tested Fuels. Long-term storage experiments were conducted using a standard heating oil extra light (HEL) according to DIN 51603-1 and a FAME from canola oil according to DIN EN 14214, as well as blends of these. Furthermore, HVO and a PtL product were examined as pure components and mixed with HEL. The compounds were blended directly before storage. The nomenclature of the blends followed in this work is listed in Table 3, along with the

https://doi.org/10.1021/acsomega.2c01970
ACS Omega 2022, 7, 26256−26264

Table 3. Overview of Examined Oils, Their Nomenclature, and Mixture Composition

fuel	HEL[a] (%)	HVO[b] (%)	FAME[c] (%)	PtL[d] (%)	stored at 8 °C	stored at 40 °C
B0	100				√	√
B10	90		10			√
B20	80		20		√	√
B20 Add1	80		20			√
B20 Add2	80		20			√
B100			100		√	√
H10	90	10			√	√
H100		100			√	√
P10	90			10		√
P100				100		√
R33	67	36	7			√

[a]HEL, heating oil extra light according to DIN 51603-1. [b]HVO, hydrogenated vegetable oil. [c]FAME, fatty acid methyl ester. [d]PtL, power-to-liquid product. Additives mixed with B20 are Add1, butylated hydroxytoluene; and Add2, a commercially available multipurpose additive.

blend compositions and storage temperatures. Two samples of B20 contained small amounts of additives in their FAME content, namely butylated hydroxytoluene (Add1) and a commercially available multipurpose additive compound (Add2) made up of antioxidants among other additives. Since additives can delay aging product formation,[7,41,42] an additive content below the recommended dosage was chosen. Also, no copper was inserted in the fuel to avoid altering the results of acid number and oxidation stability measurements.[42]

Fuel Aging Procedure. The fuels were stored for 18 months. Each of the samples mentioned in Table 3 was filled in six 1 L borosilicate glass bottles, resulting in 66 bottles. All oils were stored in a cabinet at 40 °C with the cap unscrewed to expose them to air and oxygen. A second batch containing five of the blends was stored in a refrigerator at 8 °C, totaling 96 bottles. Only selected fuels were stored at 8 °C to accommodate for the restricted available space. The bottles in the fridge were topped with an open tube filled with a drying agent to prevent water from condensing into the samples while still exposing them to air. Every 3 months, a bottle of each sample was taken out and subsequently analyzed by different techniques. During the long-term storage at 8 °C, solid precipitates were found in the bottles of pure FAME and several blends containing FAME. These were separated from the cold oil by vacuum filtration through a cellulose nitrate filter and washed with *n*-heptane. Not all the desired measurements could be performed with the precipitate owing to the very small sample amounts.

Fuel Analysis. *Standardized Methods.* All fuels were analyzed using different standard analytical methods to investigate if the fuel quality was within the range of the respective norms. Measured parameters were density (DIN EN ISO 12185), total contamination (DIN 12662:1998), storage stability (DIN 51471), thermal stability (DIN 51371), oxidation stability (PetroOxy method DIN 16091 and Rancimat method DIN EN 15751), acid number (DIN EN 14104), and water content (Karl Fischer method DIN EN ISO 12937). Additionally, the fuels were inspected photographically before the analyses. For this, the bottles were photographed in a well-lit photo booth, always using identical camera equipment and settings and focusing on the same point in space.

Nuclear Magnetic Resonance (NMR). Oils were examined biweekly by ^{1}H NMR spectroscopy with a Spinsolve 40 Carbon benchtop spectrometer from Magritek (Aachen, Germany) working at a proton frequency of 43 MHz. One milliliter of oil was extracted from the same bottle stored for 18 months for each NMR analysis and filled into a standard 5 mm outer diameter NMR tube. Since the spectrometer utilizes an external reference, no solvent or reference substance had to be added. Each spectrum was acquired using 40 scans and a repetition time of 15 s, which is a waiting time more than sufficient to ensure quantitative data according to ^{1}H spin−lattice T_1 relaxation measurements (T_1 < 2 s for all functional groups). Spectra were referenced to the prominent CH_2 peak and normalized to account for density changes. Series of integral data were tested for outliers using a Dean−Dixon test with a significance level of >99%. Afterward, a Neumann trend test was applied to spot a significant trend in the data. For the precipitate sample of B100, a high-field ^{1}H NMR spectrum was acquired on a Bruker Avance 400 MHz spectrometer using the standard zg30 pulse sequence and deuterated chloroform as the solvent.

Thermogravimetric Analysis (TGA). Precipitate samples from B100 stored at 8 °C were analyzed regarding their vaporization and thermal degradation behavior, and this was compared to the behavior of the corresponding heating oil samples. The analyses were conducted in a Mettler-Toledo TGA 2 device (Gießen, Germany), with which the temperature was increased from 20 to 500 °C with a 5 K min^{-1} heating rate in oxygen or nitrogen atmosphere. Similar precipitates were found in B20, but the amount was too low to conduct TGA.

Differential Scanning Calorimetry (DSC). Precipitates from the long-term storage of B20 and B100 were examined by DSC and compared to a thermogram of commercially available paraffin. Measurements were performed on a DSC 200 F3 Maia calorimeter from NETZSCH (Selb, Germany). Samples were heated at 20 K min^{-1} from 25 to 200 °C with a constant nitrogen purge of 20 mL min^{-1} twice, with a cooling rate of 20 K min^{-1} between both heating cycles.

Two-Dimensional Gas Chromatography with Mass Spectrometry (2D-GC-MS). 2D-GC-MS measurements of the precipitate from B100 were conducted by ASG Analytik-Service AG (Neuss, Germany) using their method, ASG 2253 GCxGC-MS. Usually, when middle distillates are measured, 500 μL of the sample is mixed with internal standards and diluted with dichloromethane. Because only a small amount of precipitate was available, only 28 mg was dissolved in dichloromethane. Then, 1 μL of the solution was injected on-column for the measurement. The two consecutive columns separated the components by their carbon chain length and polarity.

Attenuated Total Reflection Fourier-Transform Infrared Spectroscopy (ATR-FTIR). Infrared spectra were acquired with a Spectrum Two spectrometer from PerkinElmer (Waltham, MA). Samples were deposited on the ATR crystal and covered to prevent CO_2 from the operator's breath from dissolving in the sample. Sixty-four scans were accumulated in a spectral range from 450 to 4000 cm^{-1}.

https://doi.org/10.1021/acsomega.2c01970
ACS Omega 2022, 7, 26256−26264

■ ASSOCIATED CONTENT

Supporting Information

The Supporting Information is available free of charge at https://pubs.acs.org/doi/10.1021/acsomega.2c01970.

Compilation of photos, results from standard methods, NMR, and IR (PDF)

■ AUTHOR INFORMATION

Corresponding Author

Alina Adams − *Institut für Technische und Makromolekulare Chemie, RWTH Aachen University, 52074 Aachen, Germany;* orcid.org/0000-0002-0892-6399; Email: Alina.Adams@itmc.rwth-aachen.de

Authors

Karin Engeländer − *OWI Science for Fuels gGmbH, RWTH Aachen University, 52134 Herzogenrath, Germany*

Anton Duchowny − *Institut für Technische und Makromolekulare Chemie, RWTH Aachen University, 52074 Aachen, Germany;* orcid.org/0000-0002-3159-3561

Bernhard Blümich − *Institut für Technische und Makromolekulare Chemie, RWTH Aachen University, 52074 Aachen, Germany*

Complete contact information is available at: https://pubs.acs.org/10.1021/acsomega.2c01970

Notes

The authors declare no competing financial interest.

■ ACKNOWLEDGMENTS

This IGF Project number 18951 N/1 was supported by the DGMK under the number 778 via the AiF within the program for promoting the Industrial Collective Research (IGF) of the German Ministry of Economic Affairs and Energy (BMWi), based on a resolution of the German Parliament.

■ REFERENCES

(1) Gustavsson, L.; Börjesson, P.; Johansson, B.; Svenningsson, P. Reducing CO2 emissions by substituting biomass for fossil fuels. *Energy* **1995**, *20*, 1097−1113.

(2) Shah, S. A. R.; Naqvi, S. A. A.; Riaz, S.; Anwar, S.; Abbas, N. Nexus of biomass energy, key determinants of economic development and environment: A fresh evidence from Asia. *Renewable and Sustainable Energy Reviews* **2020**, *133*, 110244.

(3) Fukuda, H.; Kondo, A.; Noda, H. Biodiesel fuel production by transesterification of oils. *J. Biosci. Bioeng.* **2001**, *92*, 405−416.

(4) Vyas, A. P.; Verma, J. L.; Subrahmanyam, N. A review on FAME production processes. *Fuel* **2010**, *89*, 1−9.

(5) Longanesi, L.; Pereira, A. P.; Johnston, N.; Chuck, C. J. Oxidative stability of biodiesel: recent insights. *Biofuels, Bioproducts and Biorefining* **2022**, *16*, 265−289.

(6) Schober, S.; Mittelbach, M. The impact of antioxidants on biodiesel oxidation stability. *European Journal of Lipid Science and Technology* **2004**, *106*, 382−389.

(7) Christensen, E.; McCormick, R. L. Long-term storage stability of biodiesel and biodiesel blends. *Fuel Process. Technol.* **2014**, *128*, 339−348.

(8) Bowden, F. P.; Leben, L.; Tabor, D. The influence of temperature on the stability of a mineral oil. *Trans. Faraday Soc.* **1939**, *35*, 900.

(9) Czarnocka, J.; Matuszewska, A.; Odziemkowska, M. *Storage Stability of Fuels*; Biernat, K., Ed.; IntechOpen: London, 2015; pp 157−188.

(10) Singer, A.; Schröder, O.; Pabst, C.; Munack, A.; Bünger, J.; Ruck, W.; Krahl, J. Aging studies of biodiesel and HVO and their testing as neat fuel and blends for exhaust emissions in heavy-duty engines and passenger cars. *Fuel* **2015**, *153*, 595−603.

(11) Hoang, A. T.; Le, A. T. A review on deposit formation in the injector of diesel engines running on biodiesel. *Energy Sources, Part A: Recovery, Utilization, and Environmental Effects* **2019**, *41*, 584−599.

(12) Feldhoff, S.; Eiden, S.; Staufenbiel, J.; Singer, A. *Proceedings of the 19th Internationale Stuttgarter Symposium*; Bargende, M., Reuss, H.-C., Wagner, A., Wiedemann, J., Eds.; Springer Fachmedien Wiesbaden: Wiesbaden, Germany, 2019; pp 1293−1307.

(13) Komariah, L. N.; Hadiah, F.; Aprianjaya, F.; Nevriadi, F. Biodiesel effects on fuel filter; assessment of clogging characteristics. *J. Phys.: Conf. Ser.* **2018**, *1095*, 012017.

(14) Cardeño, F.; Lapuerta, M.; Rios, L.; Agudelo, J. R. Reconsideration of regulated contamination limits to improve filterability of biodiesel and blends with diesel fuels. *Renewable Energy* **2020**, *159*, 1243−1251.

(15) Schümann, U.; Buchholz, I. B. *Deposit Formation and Prevention of Deposit Formation Biodiesel (EN 14214)*. https://www.agqm-biodiesel.de/application/files/1516/0188/5492/AGQM_Abschlussbericht_Belagsminderung_Biodiesel_31-07-2020_Final_EN.pdf.

(16) Caprotti, R.; Breakspear, A.; Klaua, T.; Weiland, P.; Graupner, O.; Bittner, M. RME Behaviour in Current and Future Diesel Fuel FIE's. *Powertrain & Fluid Systems Conference and Exhibition*; SAE Technical Paper 2007-01-3982; 2007; DOI: 10.4271/2007-01-3982.

(17) Saltas, E.; Bouilly, J.; Geivanidis, S.; Samaras, Z.; Mohammadi, A.; Iida, Y. Investigation of the effects of biodiesel aging on the degradation of common rail fuel injection systems. *Fuel* **2017**, *200*, 357−370.

(18) Feldhoff, S.; Hildebrandt, K. *Investigation and evaluation of the influences on the deposition formation in diesel injectors as well as experimentally based modelling by means of a non-engine injector deposition test bench*, 1st ed.; DGMK Deutsche Wissenschaftliche Gesellschaft für Erdöl, Erdgas und Kohle e.V.: Hamburg, Germany, 2019.

(19) Ueckerdt, F.; Bauer, C.; Dirnaichner, A.; Everall, J.; Sacchi, R.; Luderer, G. Potential and risks of hydrogen-based e-fuels in climate change mitigation. *Nature Climate Change* **2021**, *11*, 384−393.

(20) Nikolskaya, E.; Hiltunen, Y. Time-Domain NMR in Characterization of Liquid Fuels: A Mini-Review. *Energy Fuels* **2020**, *34*, 7929−7934.

(21) Förster, E.; Becker, J.; Dalitz, F.; Görling, B.; Luy, B.; Nirschl, H.; Guthausen, G. NMR Investigations on the Aging of Motor Oils. *Energy Fuels* **2015**, *29*, 7204−7212.

(22) Förster, E.; Fraenza, C. C.; Küstner, J.; Anoardo, E.; Nirschl, H.; Guthausen, G. Monitoring of engine oil aging by diffusion and low-field nuclear magnetic resonance relaxation. *Measurement* **2019**, *137*, 673−682.

(23) Mello, V. M.; Oliveira, F. C. C.; Fraga, W. G.; do Nascimento, C. J.; Suarez, P. A. Z. Determination of the content of fatty acid methyl esters (FAME) in biodiesel samples obtained by esterification using 1H-NMR spectroscopy. *Magnetic resonance in chemistry: MRC* **2008**, *46*, 1051−1054.

(24) Satyarthi, J. K.; Srinivas, D.; Ratnasamy, P. Estimation of Free Fatty Acid Content in Oils, Fats, and Biodiesel by 1 H NMR Spectroscopy. *Energy Fuels* **2009**, *23*, 2273−2277.

(25) Monteiro, M. R.; Ambrozin, A.; Lião, L. M.; Ferreira, A. G. Determination of biodiesel blend levels in different diesel samples by 1H NMR. *Fuel* **2009**, *88*, 691−696.

(26) Fraenza, C. C.; Förster, E.; Guthausen, G.; Nirschl, H.; Anoardo, E. Use of 1H-NMR spectroscopy, diffusometry and relaxometry for the characterization of thermally-induced degradation of motor oils. *Tribiol. Int.* **2021**, *153*, 106620.

(27) Singh, K.; Kumar, S. P.; Blümich, B. Monitoring the mechanism and kinetics of a transesterification reaction for the biodiesel production with low field 1H NMR spectroscopy. *Fuel* **2019**, *243*, 192−201.

(28) Duchowny, A.; Dupuy, P. M.; Widerøe, H. C.; Berg, O. J.; Faanes, A.; Paulsen, A.; Thern, H.; Mohnke, O.; Küppers, M.; Blümich, B.; Adams, A. Versatile high-pressure gas apparatus for benchtop NMR: Design and selected applications. *Journal of magnetic resonance* **2021**, *329*, 107025.
(29) Duchowny, A.; Adams, A. Compact NMR Spectroscopy for Low-Cost Identification and Quantification of PVC Plasticizers. *Molecules* **2021**, *26*, 1221.
(30) Conceição, M. M.; Fernandes, V. J.; Araújo, A. S.; Farias, M. F.; Santos, I. M. G.; Souza, A. G. Thermal and Oxidative Degradation of Castor Oil Biodiesel. *Energy Fuels* **2007**, *21*, 1522−1527.
(31) Bacha, K.; Ben-Amara, A.; Vannier, A.; Alves-Fortunato, M.; Nardin, M. Oxidation Stability of Diesel/Biodiesel Fuels Measured by a PetroOxy Device and Characterization of Oxidation Products. *Energy Fuels* **2015**, *29*, 4345−4355.
(32) Vega-Lizama, T.; Díaz-Ballote, L.; Hernández-Mézquita, E.; May-Crespo, F.; Castro-Borges, P.; Castillo-Atoche, A.; González-García, G.; Maldonado, L. Thermogravimetric analysis as a rapid and simple method to determine the degradation degree of soy biodiesel. *Fuel* **2015**, *156*, 158−162.
(33) Zhou, J.; Xiong, Y.; Gong, Y.; Liu, X. Analysis of the oxidative degradation of biodiesel blends using FTIR, UV-Vis, TGA and TD-DES methods. *Fuel* **2017**, *202*, 23−28.
(34) Brendel, K.; Duchowny, A. *Untersuchung zur Vermeidung von höhermolekularen Alterungsprodukten in Mitteldestillaten mit alternativen Komponenten unter anwendungstechnischen Randbedingungen: Investigation on avoiding high-molecular aging products in middle distillates with alternative blend components under technical conditions*; DGMK-Forschungsbericht; DGMK e.V: Hamburg, Mai, 2020; Vol. *778*.
(35) Jayalakshmi, V.; Selvavathi, V.; Sekar, M. S.; Sairam, B. Characterization of paraffin waxes by DSC and high temperature GC. *Petroleum Science and Technology* **1999**, *17*, 843−856.
(36) Hatzakis, E.; Agiomyrgianaki, A.; Kostidis, S.; Dais, P. High-Resolution NMR Spectroscopy: An Alternative Fast Tool for Qualitative and Quantitative Analysis of Diacylglycerol (DAG) Oil. *J. Am. Oil Chem. Soc.* **2011**, *88*, 1695−1708.
(37) Fang, H. L.; McCormick, R. L. Spectroscopic Study of Biodiesel Degradation Pathways. *Powertrain & Fluid Systems Conference and Exhibition, Toronto, October 16−19, 2006*; 2006; DOI: 10.4271/2006-01-3300.
(38) Singer, P.; Rühe, J. On the mechanism of deposit formation during thermal oxidation of mineral diesel and diesel/biodiesel blends under accelerated conditions. *Fuel* **2014**, *133*, 245−252.
(39) Alves-Fortunato, M.; Ayoub, E.; Bacha, K.; Mouret, A.; Dalmazzone, C. Fatty Acids Methyl Esters (FAME) autoxidation: New insights on insoluble deposit formation process in biofuels. *Fuel* **2020**, *268*, 117074.
(40) Jose, T. K.; Anand, K. Effects of biodiesel composition on its long term storage stability. *Fuel* **2016**, *177*, 190−196.
(41) Shiotani, H.; Goto, S. Studies of Fuel Properties and Oxidation Stability of Biodiesel Fuel. *2007 Fuels and Emissions Conference*; 2007. DOI: 10.4271/2007-01-0073.
(42) Yang, Z.; Hollebone, B. P.; Wang, Z.; Yang, C.; Brown, C.; Landriault, M. Storage stability of commercially available biodiesels and their blends under different storage conditions. *Fuel* **2014**, *115*, 366−377.

https://doi.org/10.1021/acsomega.2c01970
ACS Omega 2022, 7, 26256−26264